



ARTICLE

Characterization of Nanocomposite Membrane Based Bacterial Cellulose Made of Pineapple Waste Reinforced by Graphite Nanoplatelets

Heru Suryanto^{1,2,*}, Bili Darnanto Susilo³, Jibril Maulana³, Aminnudin³, Uun Yanuhar⁴,
Surjani Wonorahardjo^{2,5}, Husni Wahyu Wijaya^{2,5} and Abu Saad Ansari⁶

¹Center of Excellence for Cellulose Composite (CECCom), Department of Mechanical Engineering, Universitas Negeri Malang, Malang, 65145, Indonesia

²Centre of Advanced Material for Renewable Energy (CAMRY), Universitas Negeri Malang, Malang, 65145, Indonesia

³Master Program of Mechanical Engineering, Faculty of Engineering, Universitas Negeri Malang, Malang, 65145, Indonesia

⁴Department of Aquatic Resources Management, Faculty of Fisheries and Marine Sciences, Brawijaya University, Malang, 65145, Indonesia

⁵Department of Chemistry, Faculty of Mathematics and Natural Sciences, Universitas Negeri Malang, Malang, 65145, Indonesia

⁶Department of Materials Science & Engineering, Incheon National University, Incheon, 464-742, South Korea

*Corresponding Author: Heru Suryanto. Email: heru.suryanto.ft@um.ac.id

Received: 25 November 2021 Accepted: 25 February 2022

ABSTRACT

Waste is the main problem for the environment. Handling waste for various useful applications has a benefit for the future. This work has been studied for handling pineapple peel waste to make composite film bacterial cellulose nanocomposite membrane (BCNM) with addition graphite nanoplatelet (GNP). The concentration of GNP in the membrane influence the membrane properties. The bacterial cellulose (BC) pellicle was synthesized by using media from pineapple peel waste extract. BC pellicle is cleaned with water and NaOH solution to be free from impactors. BCNM is synthesized through the mechanical disintegration stage. The results of disintegration using high pressure homogenizer at 150 bar and five cycles. BCNM/GNP is synthesized with varying addition of GNP of 2.5, 5.0, 10 and 100 wt% of dry bacterial nanocellulose (BNC). The BC and GNP solution were dried in an oven for 14 h at 80°C. BCNM morphology was observed using SEM. GNP is dispersed and distributed in the BC matrix as reinforcement. FTIR analysis shows many peaks of BNC less pronounced with increasing of GNP. The higher concentration of GNP, the rougher of BCNM. The optimum tensile strength of BCNM was achieved after addition GNP of 2.5 wt%.

KEYWORDS

Bacterial nanocellulose; graphite nanoplatelet; membrane; nanocomposite; pineapple waste

1 Introduction

Cellulose is the most abundant natural polymer that has properties of high strength, semicrystalline, renewable, and biodegradable [1]. It is produced in trillion tons per year to supply the textile and paper industry [2]. Bacterial cellulose (BC) is cellulose material synthesized by bacteria of *Acetobacter xylinum* or *Gluconobacter xylinus* [3]. It is a hydrogel constructed from a network of three-dimensional cellulose



fibrils [4]. BC has the same properties as cellulose in plants, but it has a different degree of polymerization, three-dimensional structure, and physicochemical characteristics [5]. High crystallinity (60–80%), good mechanical characteristics, and in situ tunability are all attributes of BC cellulose chains [6]. BC has been processed as electrodes material for batteries and supercapacitors [4]. In hybrid nanocomposites, BC is also utilized as a reinforcement agent, transparent film, and binder [7]. As a result, there is a lot of promise for using bacterial nanocellulose (BNC) as a binder in energy storage devices like Li-ion battery electrodes [8,9].

Graphite nano-platelet (GNP) is carbon material which having nano-structure in the form of platelet (two-dimension material) [10] that have been used to alter electrochemical process [11], mechanical properties [2], electrical properties [12], and thermal properties [13] in BC composite [14]. The nano graphite has been used as a filling material in BC. Erbas Kiziltas et al. [15] have synthesized BC/nano-graphite composite membranes, where BC formed a continuous network throughout the BC matrix, and nano-graphite is perfectly dispersed. However, the study uses HS culture media as a fermentation medium to produce BC. Kiziltas et al. [15] also synthesis membrane of nanocellulose from kraft pulp fiber with reinforcement nano graphite and presence of carboxymethyl cellulose additive. However, the membrane source is cellulose from the plant where in the future it can cause a problem for the environment. This study used an extract of pineapple peel waste as source medium fermentation to produce BC as a way to handle pineapple peel waste and explore the properties of bacterial cellulose nanocomposite membrane (BCNM) reinforced by GNP.

2 Material and Methods

2.1 Materials

This experiment uses *Acetobacter xylinum* bacteria, and pineapple peel waste sources were collected from the people's plantation at Blitar, East Java, Indonesia. Additional chemical reagents were NaOH, urea, and glucose ($C_6H_{12}O_6$) supplied by Sigma-Aldridge, Singapore. GNP supplied by SkySpring Nanomaterials, Inc., Houston, USA.

2.2 Production of BC Pellicle

Production of BC pellicle was referred to Suryanto et al. [16]. Initially, the pineapple peels waste (300 g) was cleaned and put into a blender chamber. Add water up to a volume of 1 L, then crushed by a blender at 26,000 rpm for 1.5 min. Then add more water until the volume is 2 L and in the blender for 1 min. After that, the solution is filtered to get pineapple peels waste extract. The pineapple peel extract was boiled for sterilization. At boiling process, solution was added with 7.5% (w/v) glucose and 0.5% (w/v) urea, then chilled. The culture medium was adjusted to a pH of 4.5 using acetic acid solution (Sigma-Aldrich, Singapore). A bacterial starter, *Acetobacter xylinum* of 1% (v/v), was added into the culture medium, and then it was fermented at 30°C. After 10–14 days, the fermentation process formed pellicles that floated on the surface of the culture medium. The pellicles were taken and washed using distilled water. To remove the impurities from bacteria and the growth medium, pellicle then boiled using a solution of NaOH 1% (Sigma-Aldrich, Singapore) at 90°C for 2 h and extensively washed with distilled water at 25°C until the pH of the water was about 7.0 (neutral). Boiling with dilute alkaline solution has a limited influence on the microstructure and mechanical properties [17].

2.3 Homogenization Process

The cleaned pellicles were cut into smaller sizes and crushed using a high-speed blender (Fomac, ICH-DS7 model, China) at 26000 rpm for five minutes. BC pulp was diluted distilled water until concentration of 0.5% (w/v). The homogenization process was conducted in High-Pressure Homogenizer equipment (Berkley

Scientific, AH-100D model, China) with five cycles at 150 bar pressure. Nanocellulose results were put in a beaker glass and saved in a refrigerator chamber at 4°C for the next process.

2.4 Production of BNC

The BNC production was conducted according to previously published methods [18]. Fifty grams of BC pellicle were put into blender chamber containing distilled water of 300 mL then crushed for 1.5 min with a blender at 26,000 rpm. While in a blender, added distilled water of 700 mL and crushed for 2 min. Solution of produced BC was homogenized in high-pressure homogenizer with five cycles at a pressure of 150 bars. BNC obtained after filtering process of solution using a vacuum filter.

2.5 Synthesis of BNC/GNP Nanocomposite Membrane

Ten grams of BNC reinforced by GNP with variations of 0.0, 2.5, 5.0, 10 and 100 wt% of dry BNC were diluted in 200 mL of purified water. The solution was stirred for 45 min. After that, the solution was sonicated for 20 min using an ultrasonic homogenizer. The sonication results were put on an aluminium-paper-coated glass mold and dried in an oven for 14 h at 80°C [19].

2.6 Surface Morphology Analysis

Microscope (SEM) (FEI, Inspect-S50, Japan) with an operating voltage of 30.00 kV was used for surface observation. Specimen's surface was treated by gold coating (SC7-620 Emitech sputter coater, UK) before observation. ImageJ 1.52a software was used to analyse SEM photograph images to obtain BNC fiber diameters. The measurement of fiber diameter was performed 25 times at random fiber in the SEM photograph.

2.7 FTIR Analysis

The function group was analyzed using the FTIR Shimadzu IR Prestige-21 Spectrum. 0.1 mg BCNM samples were ground into powder, mixed with 1 mg KBr powder, and pressed to become a pellet. FTIR spectra were recorded with a step of 2 cm⁻¹ in the wavenumber of 400–4000 cm⁻¹.

2.8 XRD Analysis

The BCNM structure was analyzed by XRD (PANalytical XPert PRO, USA). The scanning of BCNM was done with a diffraction angle from 10° to 70° with CuK α radiation ($\lambda = 1.54 \text{ \AA}$) at 30 mA and 40 kV. The crystallite size of BCNM was calculated using the Scherrer formula.

2.9 Mechanical Properties Test

The tensile strength and elongation at breaks were analysed using tensile test equipment (Techno Lab., Indonesia) with a rate of 0.025 mm.s⁻¹. The sample dimension referred to ASTM D638-V standard Tensile test, and testing was performed three times.

2.10 Surface Roughness Test

The BCNM surface was observed using a portable surface tester (Surftest SJ-301 type, Mitutoyo Co., Japan) with 0.75 mN gauge precision and 0.8 mm λc profile filter. The roughness average (Ra) was measured with the rate of 5.0 $\mu\text{m.cm}^{-1}$ in a vertical direction, 200.0 $\mu\text{m.cm}^{-1}$ in a horizontal direction and 4 mm of total measurement length. Measurement was conducted in three repetitions.

3 Result and Discussion

3.1 Morphology Observation

The surface observations of BC membrane and BCNM are shown in Figs. 1 and 2, respectively. BNC membrane is synthesized through the fibrillation process in HPH that results in nano-sized cellulose. Fig. 1

shows the morphology of the BNC membrane observed using SEM at a magnification of 20,000 times. BC membrane has fiber diameter of 61.7 ± 36.98 , and after fibrillation process using HPH with five cycles at 150 bar, BNC membrane has fiber diameter of 53.24 ± 27.05 nm. Reducing the diameter of BC through the process of fibrillation and homogenization makes the increasing surface area of BNC so having high interaction possibility between BNC and GNP to get a good nanocomposite membrane.

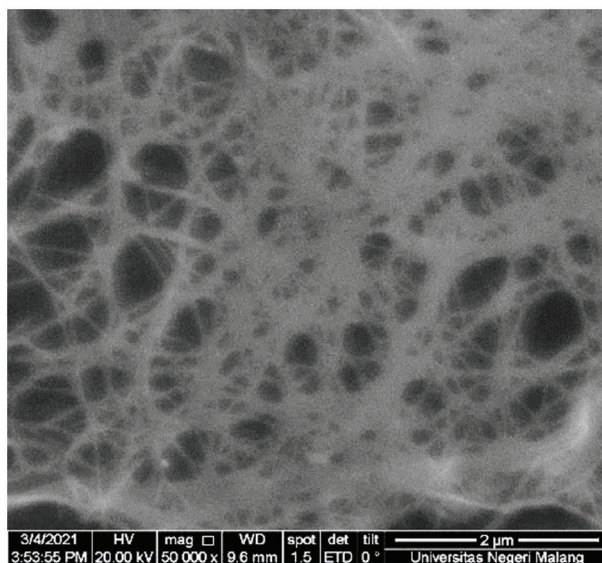


Figure 1: SEM micrographs from pure BNC membrane

An SEM micrograph of a BCNM sample is shown in Fig. 2. The BNC matrix contains GNP, which functions as a scattered filler. GNP tends to clump when dispersed in a water-based solution and forms a thicker layer on the interface [20]. The larger the amount of GNP, the larger the GNP clumping. As shown in Fig. 2A, a small addition of GNP into BCN indicate a little GNP agglomerate. Almost of GNP merge with BCN results smoother surface. Increasing the addition of GNP shows that BNC fibers can not combine well, so GNP starts to embed on the surface of BCNM (Figs. 6B–6D) to form the GNP agglomerate. The highest concentration of GNP shows many GNP agglomerate on the BCNM surface (Figs. 6E–6F). It indicates that overconcentration of GNP make agglomeration in BNC.

3.2 FTIR Analysis

The IR spectrum of the BCNP reinforced by GNP is presented in Fig. 3. There is some difference between control and BCNM. In the region of $3200\text{--}3400\text{ cm}^{-1}$, the O–H group, which is a hydroxyl group, is engaged in intramolecular and intermolecular hydrogen bonding. The amount of O–H bonds observed in the region of 3400 cm^{-1} decreases as the proportion of GNP increases. Due to the existence of CH and CH₂ groups in cellulose, there is a peak at 2895 cm^{-1} that corresponds to the C–H stretch. At 1605 cm^{-1} , a peak corresponding to the C=C bond emerges, suggesting that GNP has entered the composite film [21]. This peak becomes less pronounced as the percentage of GNP in composite films increases. The C–O group in the wavenumber of 1043 cm^{-1} decrease and shift slightly when the GNP concentration is increased.

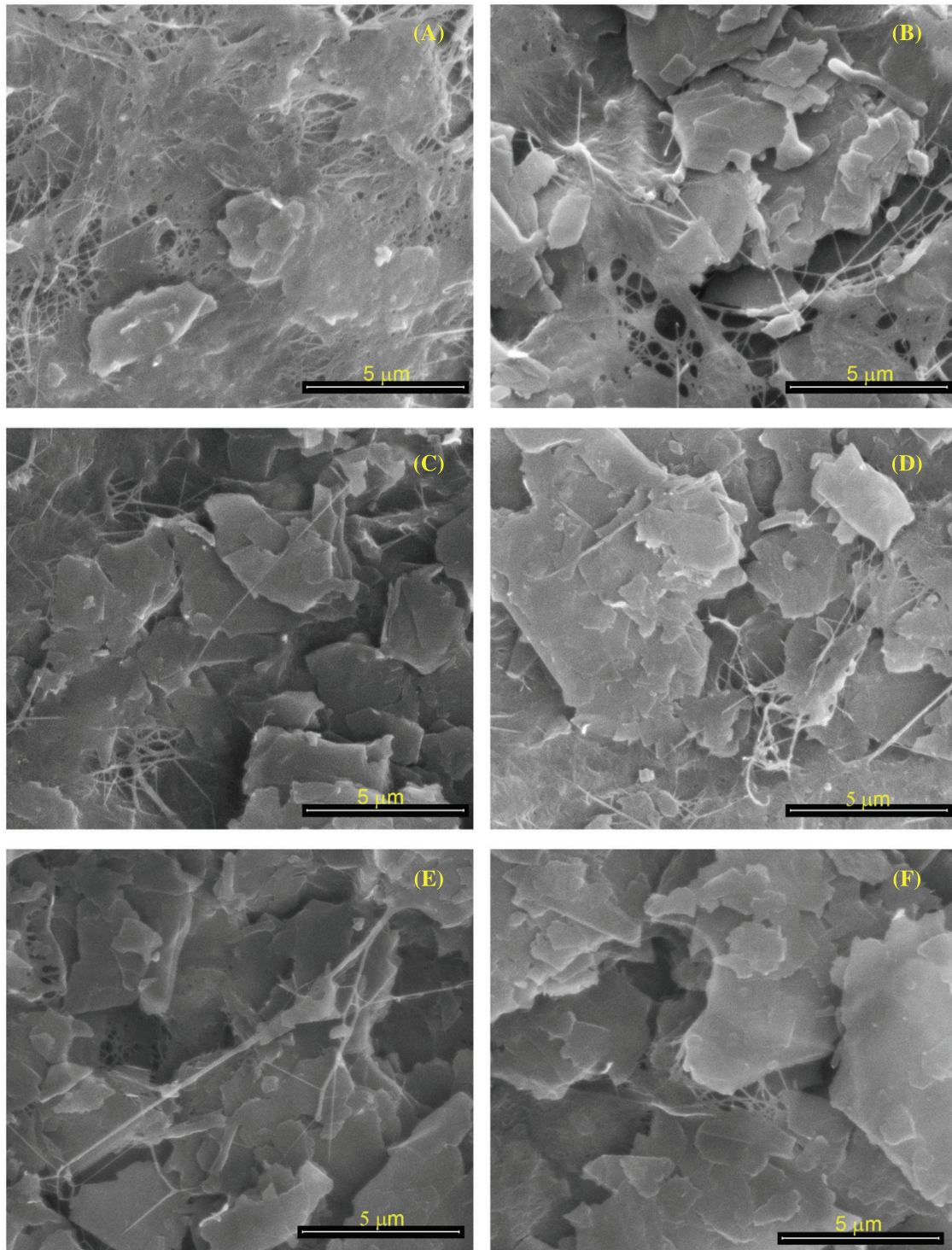


Figure 2: SEM observations of BCNM morphology with the addition GNP of (A) 2.5 wt%; (B) 5 wt%; (C) 7.5 wt%; (D) 10 wt%; (E) 50 wt%, (F) 100 wt% of dry BNC

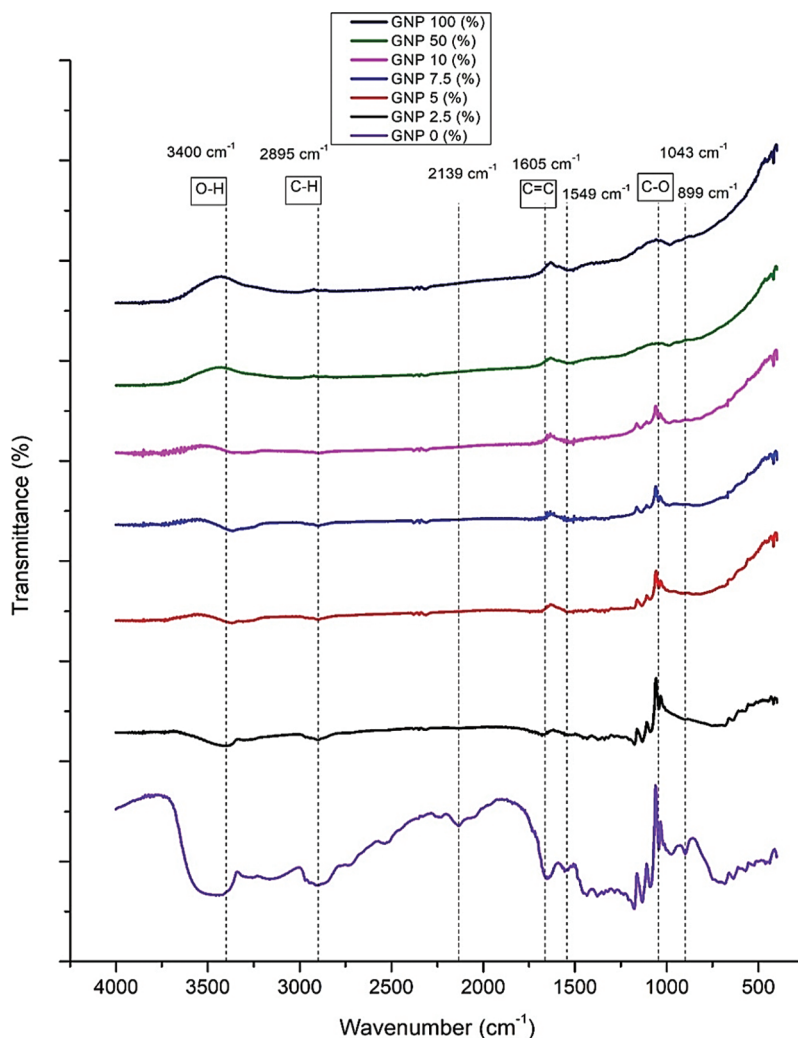


Figure 3: IR spectra of BCNM with addition GNP (wt% of dry BCN)

GNP tends to clump when dispersed in a water-based solution and form a thicker layer on the interface [22]. The high surface energy of hydroxyl groups on nanocellulose's surface causes inadequate wetting and poor interface adhesion with hydrophobic polymers [23]. This situation shows that there is no covalent or strong connection between GNP and BNC. However, incorporating GNP into BNC matrix can transform BCNM structure into a conductive membrane.

3.3 XRD Analysis

The X-ray diffractogram of the BCNM sample is shown in Fig. 4. The peak of BC is indicated at 2θ of 14.5° , 22.5° , 26.5° , and 54.6° . The peak of 2θ at 14.5° , 22.5° are corresponding to the cellulose crystalline plane of 110, and 002 [24]. The presence of a graphite structure is indicated by the peak 2θ at 26.5° , and 54.6° . The higher GNP content results in higher peak intensity of GNP into the BNC matrix. The crystalline size of the composite films for control, GNP concentration of 2.5, 5.0, 7.5, 10.0, 50, and 100 wt% are 17.2, 17.1, 14.7, 10.3, 10.3, 17.2, and 41.2 nm, respectively. Smaller crystallite sizes indicate that BC was capable of dispersing GNP particles. At high concentrations, the BCNM with high content of GNP when analyzed by XRD, the crystallite size was considered to be dominated by GNP.

At low content of GNP, the crystallites size was influenced by BC. It was confirmed by the surface morphology of BCNP at concentrations of 10 to 100 wt%, as presented in Fig. 2. The previously published study also indicate that nano-graphite and graphite have the same diffraction pattern in the region $2\theta = 26.67^\circ$ [10]. The BNC/GNP composite films also have the same peak because of GNP existence. Similar results have also been reported by Aritonang et al. [10].

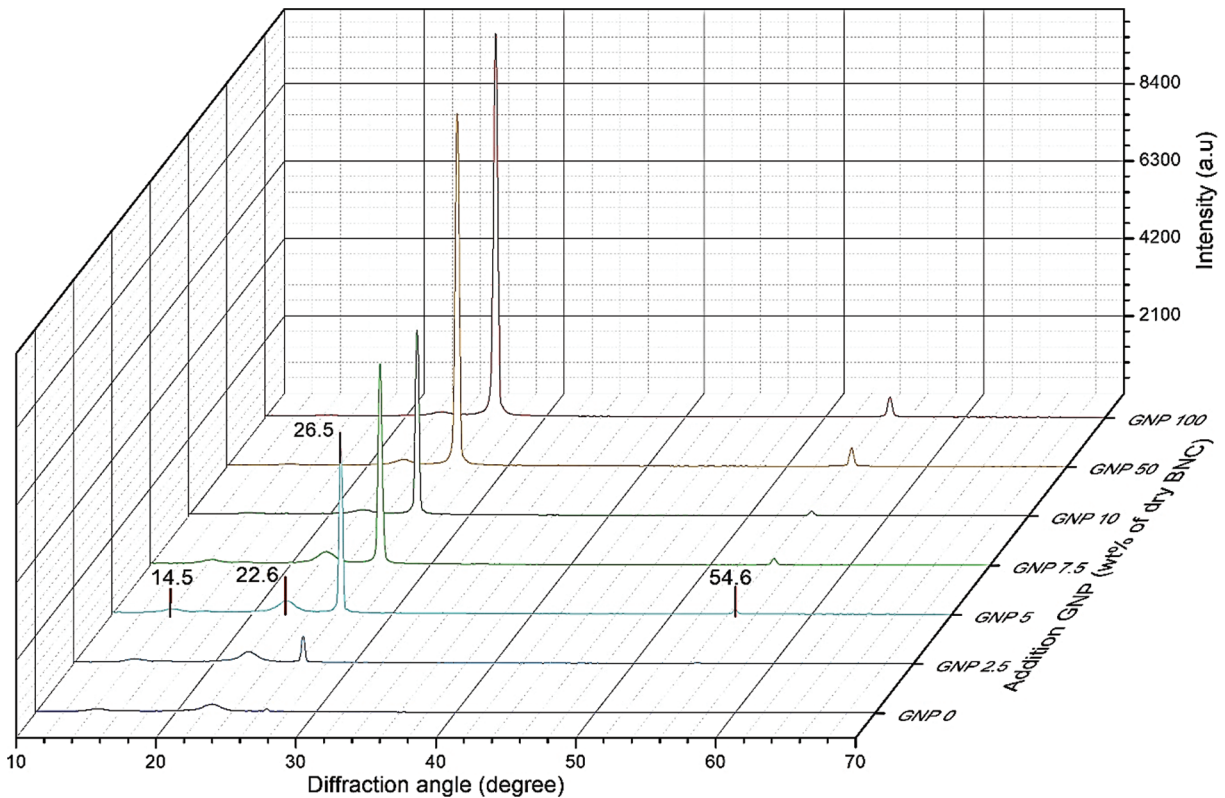


Figure 4: X-ray diffractogram of BCNM with addition of GNP of 0 (control), 2.5, 5, 7.5, 10, 50, and 100 wt% of dry BNC

3.4 Surface Roughness

The surface roughness profile of nanocomposite membrane with different content of GNP is shown in Fig. 5. Measurement quantitatively of surface roughness are shown in Fig. 6. The surface profile indicates that the addition of GNP changes the surface morphology. It can be observed that nanocomposite membrane has a different roughness and after addition to GNP. The average roughness (R_a) of BCNM with GNP concentration of 0, 2.5, 5.0, 7.5, 10, 50, and 100 wt% are $1.14 \pm 0.15 \mu\text{m}$, $1.52 \pm 0.13 \mu\text{m}$, $1.26 \pm 0.16 \mu\text{m}$, $1.06 \pm 0.15 \mu\text{m}$, $1.32 \pm 0.04 \mu\text{m}$, $1.69 \pm 0.25 \mu\text{m}$, and $2.48 \pm 0.38 \mu\text{m}$, respectively (Fig. 6).

The R_a for the BCNM without GNP is $1.14 \pm 0.15 \mu\text{m}$ with a surface profile smoother (Fig. 5A). After the GNP addition of 2.5 wt%, the surface profile of BCNM is rougher (Fig. 5B) with R_a value of $1.52 \pm 0.13 \mu\text{m}$. Increasing GNP of 5.0 wt% cause membrane surface profile to be smooth (Fig. 5C). The surface profile of 7.5 wt% GNP is the best surface profile with the lowest roughness (Fig. 5D) with R_a of $1.06 \pm 0.15 \mu\text{m}$. This result is in accord with morphology results that indicate the pore of BC is covered by GNP (Fig. 2C). Higher content GNP 10 wt% of the BCNM cause surface profile rougher with R_a of

$1.32 \pm 0.04 \mu\text{m}$ (Fig. 5E). Addition GNP 50 wt% and 100 wt% results in R_a of $1.69 \pm 0.25 \mu\text{m}$ and $2.48 \pm 0.38 \mu\text{m}$ (Figs. 5F, 5G), respectively. When the mass concentration of GNP is high, the surface pore size and pore density are covered with GNP. GNP's high content makes BCNM unable to accommodate all GNP, so GNP is deposited abundantly on the BCNM surface (Fig. 2F).

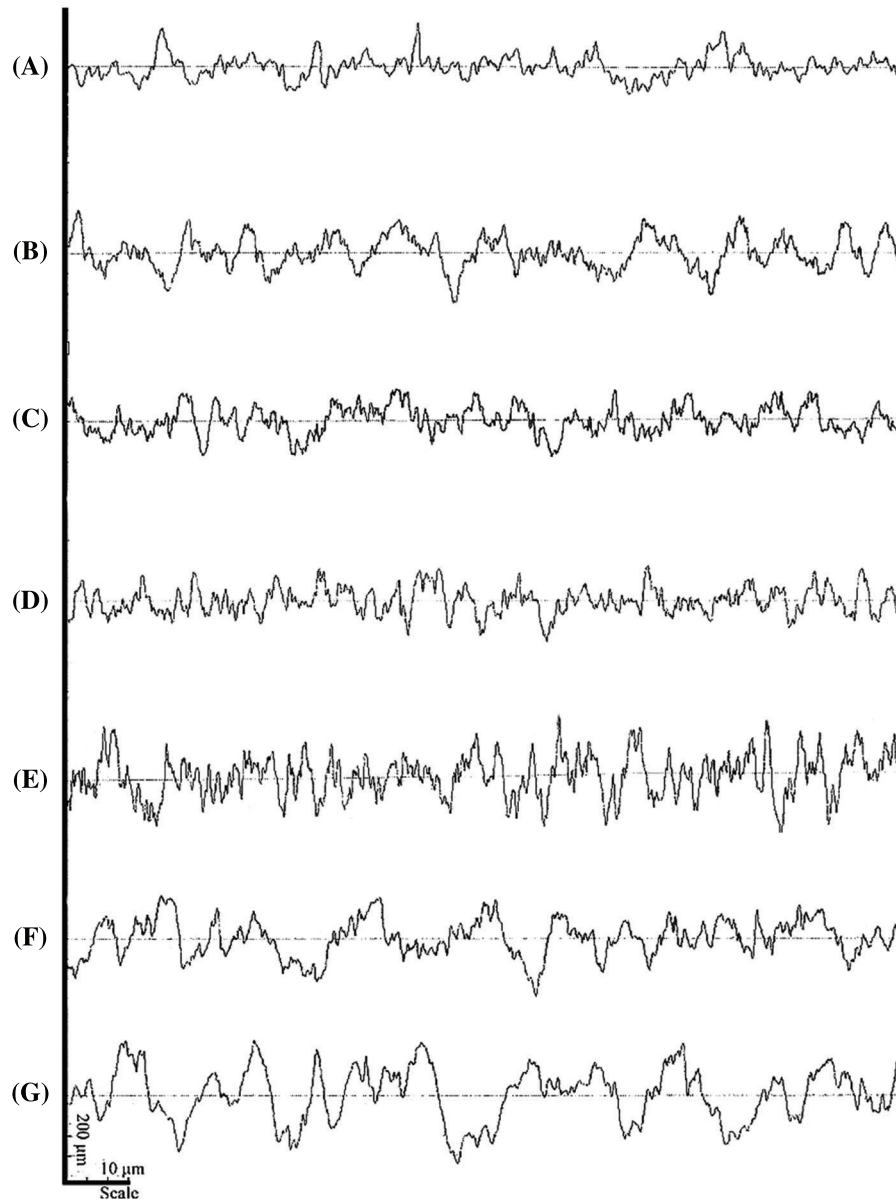


Figure 5: Surface roughness profile of BCNM with addition GNP of (A) 0 wt%, (B) 2.5 wt%, (C) 5.0 wt%, (D) 7.5 wt%, (E) 10 wt%, (F) 50 wt%, and (G) 100 wt% of dry BNC

The properties of BCNM obtained from suspension largely depend on the dispersion of GNP in the suspension. The prepared BCNM showed different roughness due to the randomly arranged GNP structure caused by rearrangement and self-assembly of the concentrated nanocellulose, thus resulting in different morphology. This finding is corroborated by the opinion of Trace et al. [25] where the

morphology product of nanocellulose depend on the possible pre- or post-treatments like drying condition and humidification as well as processing conditions [25,26].

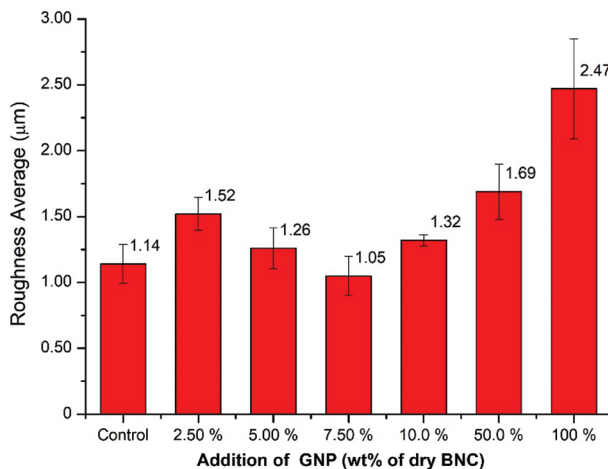


Figure 6: Surface roughness average (Ra) of BCNM with addition GNP of 0, 2.5, 5.0, 7.5, 10, 50, and 100 wt% of dry BNC

3.5 Mechanical Properties

The tensile strength and elongation at break of BCNM are shown in Fig. 7. It shows that the concentration of GNP changes the tensile strength of the membrane. The highest tensile strength (121.04 MPa) was obtained at 2.5wt% of GNP. After that, increased GNP concentration reduced the tensile strength of BCNM. Compared with BC membrane, with the addition GNP of 2.5 wt%, the tensile strength of BCNM rises about 300%. The same trend also occurs in the value of elongation at break. Elongation at break shows the highest value (3.72%) at the addition of 2.5wt% of GNP.

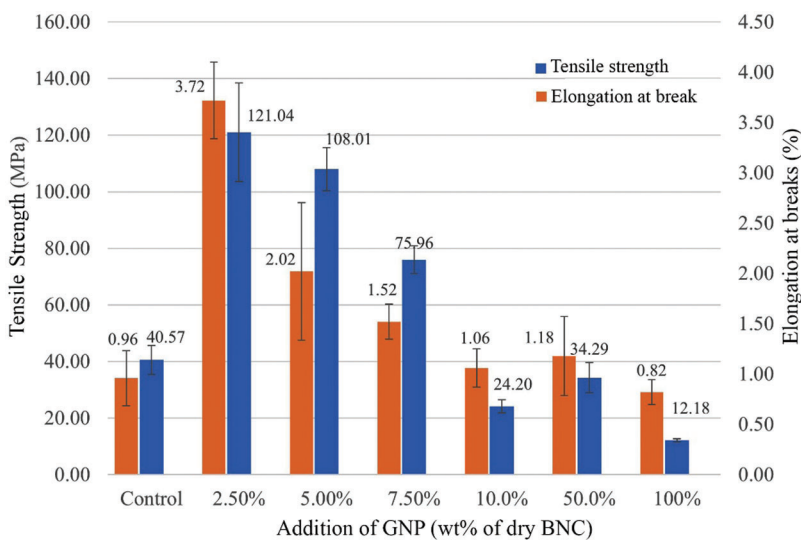


Figure 7: Mechanical properties of BCNM with addition GNP of 0, 2.5, 5.0, 7.5, 10, 50, and 100 wt% of dry BNC

At low concentrations, BNC is able to enter among GNP platelets so that GNP is intercalated, but at higher concentrations, GNP is slightly intercalated because BCN cannot enter to all of GNP platelets. Intercalated GNP has function as reinforcement of BCNM on mechanical strength. Higher concentration of GNP, the strength of BCNM is reduced, and the lowest strength is the highest concentration of GNP. A previously reported study indicates that the addition of higher GNP gradually induced cellulose crystalline conformation, affecting the swelling ability and mechanical properties [10,27].

4 Conclusion

The BCNM reinforced by GNP has been successfully produced. GNP is dispersed and distributed in the BC matrix. FTIR analysis shows many peaks of BNC less pronounced with increasing of GNP. The higher concentration of GNP, the rougher of BCNM. The maximum tensile strength of BCNM was achieved in GNP presence of 2.5 wt% with a value of 121.04 MPa. The higher of GNP content, the reducer of tensile strength. The BCNM surface profile with 7.5 wt% GNP is the best surface profile with the lowest roughness with Ra of $1.06 \pm 0.15 \mu\text{m}$. This result is in accord with morphology results that indicate the pore of BC is covered by GNP. In the future, BCNM material will develop as a conductive electrode for flexible energy devices.

Funding Statement: Author acknowledges the funding support by the Universitas Negeri Malang through the PNBPN Research Grant 2021 with PUI/CAMRY scheme by Contract No. 5.3.837/UN32.14.1/LT2021.

Conflicts of Interest: The authors declare that they have no conflicts of interest to report regarding the present study.

References

1. Ng, L. Y., Wong, T. J., Ng, C. Y., Amelia, C. K. M. (2021). A review on cellulose nanocrystals production and characterization methods from *Elaeis guineensis* empty fruit bunches. *Arabian Journal of Chemistry*, 14(9), 103339. DOI 10.1016/j.arabjc.2021.103339.
2. Yi, Z., Ren, Y., Jaffer, S., Tjong, J., Sarshar, Z. et al. (2021). Facile fabrication of electrically conductive graphitic cellulose for lighting and energy devices. *Composites Part B: Engineering*, 207, 108593. DOI 10.1016/j.compositesb.2020.108593.
3. Iguchi, M., Yamanaka, S., Budhiono, A. (2000). Bacterial cellulose—a masterpiece of nature's arts. *Journal of Materials Science*, 35(2), 261–270. DOI 10.1023/A:1004775229149.
4. Illa, M. P., Khandelwal, M., Sharma, C. S. (2018). Bacterial cellulose-derived carbon nanofibers as anode for lithium-ion batteries. *Emergent Materials*, 1(3–4), 105–120. DOI 10.1007/s42247-018-0012-2.
5. Melliawati, R., Djohan, A. C. (2013). Analysis of carboxymethyl cellulose from *acetobacter xylinum* and *acetobacter* sp. RMG-2 bacteria. *Berita Biologi*, 12(3), 335–344. DOI 10.14203/beritabiologi.v12i3.642.
6. Römling, U., Galperin, M. Y. (2015). Bacterial cellulose biosynthesis: Diversity of operons, subunits, products, and functions. *Trends in Microbiology*, 23(9), 545–557. DOI 10.1016/j.tim.2015.05.005.
7. Juntaro, J., Pommet, M., Mantalaris, A., Shaffer, M., Bismarck, A. (2007). Nanocellulose enhanced interfaces in truly green unidirectional fibre reinforced composites. *Composite Interfaces*, 14(7–9), 753–762. DOI 10.1163/156855407782106573.
8. Dutta, S., Kim, J., Ide, Y., Kim, J. H., Hossain, M. S. A. et al. (2017). 3D network of cellulose-based energy storage devices and related emerging applications. *Materials Horizons*, 4(4), 522–545. DOI 10.1039/C6MH00500D.
9. Sabo, R., Yermakov, A., Law, C. T., Elhajjar, R. (2016). Nanocellulose-enabled electronics, energy harvesting devices, smart materials and sensors: A review. *Journal of Renewable Materials*, 4(5), 297–312. DOI 10.7569/JRM.2016.634114.
10. Aritonang, H. F., Wulandari, R., Wuntu, A. D. (2020). Synthesis and characterization of bacterial cellulose/nanographite nanocomposite membranes. *Macromolecular Symposia*, 391(1), 1900145. DOI 10.1002/masy.201900145.

11. Li, Y., Sun, Z., Liu, D., Lu, S., Li, F. et al. (2020). Bacterial cellulose composite solid polymer electrolyte with high tensile strength and lithium dendrite inhibition for long life battery. *Energy & Environmental Materials*, 21(4), 434–443. DOI 10.1002/eem2.12122.
12. Zhou, T., Chen, D., Jiu, J., Nge, T. T., Sugahara, T. et al. (2013). Electrically conductive bacterial cellulose composite membranes produced by the incorporation of graphite nanoplatelets in pristine bacterial cellulose membranes. *Express Polymer Letters*, 7(9), 756–766. DOI 10.3144/expresspolymlett.2013.73.
13. Perets, Y., Aleksandrovych, L., Melnychenko, M., Lazarenko, O., Vovchenko, L. et al. (2017). The electrical properties of hybrid composites based on multiwall carbon nanotubes with graphite nanoplatelets. *Nanoscale Research Letters*, 12, 406. DOI 10.1186/s11671-017-2168-8.
14. Tayeb, A., Amini, E., Ghasemi, S., Tajvidi, M. (2018). Cellulose nanomaterials—binding properties and applications: A review. *Molecules*, 23(10), 2684. DOI 10.3390/molecules23102684.
15. Kiziltas, E. E., Kiziltas, A., Rhodes, K., Emanetoglu, N. W., Blumentritt, M. et al. (2016). Electrically conductive nano graphite-filled bacterial cellulose composites. *Carbohydrate Polymers*, 136, 1144–1151. DOI 10.1016/j.carbpol.2015.10.004.
16. Suryanto, H., Sutrisno, T. A., Muhajir, M., Zakia, N., Yanuhar, U. (2018). Effect of peroxide treatment on the structure and transparency of bacterial cellulose film. *MATEC Web of Conferences*, 204, 05015. DOI 10.1051/mateconf/201820405015.
17. Chen, S. Q., Meldrum, O. W., Liao, Q., Li, Z., Cao, X. et al. (2021). The influence of alkaline treatment on the mechanical and structural properties of bacterial cellulose. *Carbohydrate Polymers*, 271, 118431. DOI 10.1016/j.carbpol.2021.118431.
18. Sardjono, S. A., Suryanto, H., Aminudin, A., Muhajir, M. (2019). Crystallinity and morphology of the bacterial nanocellulose membrane extracted from pineapple peel waste using high-pressure homogenizer. *AIP Conference Proceedings*, 2120(1), 080015. DOI 10.1063/1.5115753.
19. Serag, E., El Nemr, A., El-Maghraby, A. (2017). Synthesis of highly effective novel graphene oxide-polyethylene glycol-polyvinyl alcohol nanocomposite hydrogel for copper removal. *Journal of Water and Environmental Nanotechnology*, 2(4), 223–234. DOI 10.22090/JWENT.2017.04.001.
20. Pogorelova, N., Rogachev, E., Digel, I., Chernigova, S., Nardin, D. (2020). Bacterial cellulose nanocomposites: Morphology and mechanical properties. *Materials*, 13(12), 2849. DOI 10.3390/ma13122849.
21. Zhang, L., Yu, Y., Zheng, S., Zhong, L., Xue, J. (2021). Preparation and properties of conductive bacterial cellulose-based graphene oxide-silver nanoparticles antibacterial dressing. *Carbohydrate Polymers*, 257, 117671. DOI 10.1016/j.carbpol.2021.117671.
22. Alberts, M., Kalaitzidou, K., Melkote, S. (2009). An investigation of graphite nanoplatelets as lubricant in grinding. *International Journal of Machine Tools and Manufacture*, 49(12–13), 966–970. DOI 10.1016/j.ijmachtools.2009.06.005.
23. Dufresne, A., Belgacem, M. N. (2013). Cellulose-reinforced composites: From micro-to nanoscale. *Polimeros*, 23(3), 277–286. DOI 10.4322/polimeros.2010.01.001.
24. Suryanto, H., Muhajir, M., Susilo, B. D., Pradana, Y. R. A., Wijaya, H. W. et al. (2021). Nanofibrillation of bacterial cellulose using high-pressure homogenization and its films characteristics. *Journal of Renewable Materials*, 9(10), 1717–1728. DOI 10.32604/jrm.2021.015312.
25. Trache, D., Tarchoun, A. F., Derradji, M., Hamidon, T. S., Masruchin, N. et al. (2020). Nanocellulose: From fundamentals to advanced applications. *Frontiers in Chemistry*, 8, 392. DOI 10.3389/fchem.2020.00392.
26. Brett, C. J., Mittal, N., Ohm, W., Gensch, M., Kreuzer, L. P. et al. (2019). Water-induced structural rearrangements on the nanoscale in ultrathin nanocellulose films. *Macromolecules*, 52(12), 4721–4728. DOI 10.1021/acs.macromol.9b00531.
27. Kiangkitiwan, N., Srikulkit, K. (2021). Preparation and properties of bacterial cellulose/graphene oxide composite films using dyeing method. *Polymer Engineering & Science*, 61(6), 1854–1863. DOI 10.1002/pen.25706.